

A Novel Electrooptical Proximity Sensor for Robotics: Calibration and Active Sensing

Adi Bonen, Ricardo E. Saad, Kenneth Carless Smith, *Life Fellow, IEEE*, and Beno Benhabib, *Member, IEEE*

Abstract—An electrooptical proximity sensor capable of measuring the distance and two-dimensional orientation of an object's surface is presented. The robustness of the sensor, targeted for utilization in robotic active sensing, is achieved via the development of a novel amplitude-modulated-based electrooptical transducer, an electronic-interface circuit that provides very good noise immunity and a wide dynamic operating range, and an effective multiregion calibration process that significantly improves pose-estimations at near proximities. An experimental setup was designed and implemented for the development and verification of the proposed proximity sensor in a simulated robotic environment. Experimental results using a variety of calibrated surfaces and materials are presented and discussed. It is shown that average accuracies of 0.01 mm and 0.03° can be achieved. The robustness of the proximity sensor is also verified for potential use in grasping objects with *a priori* noncalibrated surfaces.

I. INTRODUCTION

ROBOTIC MANIPULATORS working in complex and dynamic environments can adapt to the imprecise features of their evolving surroundings by employing various sensors. These sensors can be categorized into three groups: medium-range (proximity and recognition), short-range (proximity), and tactile (force distribution and recognition) [1], [2].

Proximity sensors bridge between medium-range sensors that provide gross pose (position and orientation) estimates of an object and tactile sensors that provide contact information. The range of proximity sensors must be sufficiently large to compensate for uncertainties in the medium-range proximity-estimation process, while having sufficient resolution and accuracy to permit effective grasping of the object.

Despite their great variety, however, proximity transducers and their accompanying electronic circuits (comprising the proximity sensor) cannot presently meet the stringent requirements of industrial robotic applications. Novel sensing algorithms and techniques still have to be employed in order

Manuscript received August 9, 1995; revised April 11, 1996. This work was supported by the Natural Sciences and Engineering Research Council of Canada. This paper was recommended for publication by Associate Editor R. Howe and Editor S. Salcudean upon evaluation of the reviewers' comments.

A. Bonen, R. E. Saad, and K. C. Smith are with the Department of Electrical and Computer Engineering, Computer Integrated Manufacturing Laboratory, University of Toronto, Toronto, Ont., M5S 3G8 Canada.

B. Benhabib is with the Department of Mechanical and Industrial Engineering, Computer Integrated Manufacturing Laboratory, University of Toronto, Toronto, Ont., M5S 3G8 Canada.

Publisher Item Identifier S 1042-296X(97)01395-5.

to improve upon current characteristics, and, furthermore, to control both the sensing and grasping processes.

In this paper, a new amplitude-modulation(AM)-based proximity sensor, which combines several novel features, is presented. The primary objective of the development was to obtain a robust proximity sensor for utilization in robotic active sensing. The sensor's strengths are based on: 1) a robust proximity transducer, described in Section II; 2) a practical electronic interface circuit which extends the sensor's dynamic measurement range, described in Section III; and 3) a novel calibration technique, described in Section IV. The potential application of the proposed sensor in controlling the micromovements of a robot's gripper is addressed in Section V.

II. PROXIMITY TRANSDUCER

Transducers used by current proximity sensors vary in sophistication. Although a large variety of such transducers have already been proposed and built, new and improved transducer types are commonly reported in the literature. Various transduction media are used for proximity-sensing, including sound waves, magnetic fields, electric fields, and light (employing electrooptics) [3]. For various reasons (including the smaller size of the sensor head, the required range of operation, and the lack of moving parts), the electrooptical schemes are more suited for use in proximity sensors intended to reside on a robotic gripper, and thus are more commonly reported in the literature.

Conventionally, electrooptical proximity sensors have utilized one of two methods of operation, involving: the triangulation principle, or the light-intensity-modulation principles AM or phase modulation (PM). Triangulation schemes are usually more robust than AM and PM schemes, since they are not directly susceptible to variations in light-reflection intensity. They are well suited for medium-range localization tasks, [5].

In contrast, AM and PM sensors are more susceptible to variations in surface-reflection characteristics, and their accuracy at large distances is relatively low. However, in the case of AM sensors, distance sensitivity of the sensor is related to the distance squared [6]. Thus, these sensors are well-suited for active-sensing during grasping tasks, where continuous measurements taken during the closing-in motion can be used to increase the accuracy of the surface-pose estimation. Active sensing using AM proximity sensors was suggested previously

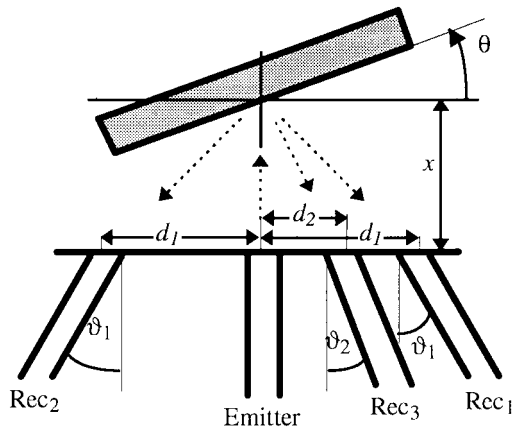


Fig. 1. A typical (fiber-optic-cable) receiver-pair constellation for distance and orientation measurement.

for applications such as: alignment of components in precision assembly [7], [8], one-dimensional (distance) handling of contact/noncontact transitions [9], and one-dimensional (distance) robot-end-effect position control [10], [11]. Thus, the AM scheme was chosen for the development of the transducer proposed herein.

A. Amplitude-Modulation Transduction

An AM transducer usually consists of one emitter and several receivers (Fig. 1). The signal amplitude at each detector is a function of all the sensor's geometrical parameters, the reflectivity characteristics of the object's surface, and its pose. Thus, the surface pose can be deduced when sufficient knowledge exists about the other parameters. In any measurement, at least two detectors are used in order to compensate for changes in various parameters, such as light-source intensity, and surface reflectivity [6], [12].

Geometrical design of the AM transducer and its receivers is based generally on the symmetry property. The measurement of surface orientation can greatly benefit from a symmetrical constellation, while distance-measurement requires asymmetry in the configuration of the receivers relative to the emitter. The three receivers of the basic AM proximity transducer in Fig. 1 can therefore be used for measuring both distance (with pair Rec₁-Rec₃) and orientation (with pair Rec₁-Rec₂).

The light intensity at the receiver as a function of the surface orientation is illustrated in Fig. 2(a). The shape of this graph is governed primarily by the surface's angular-reflectance profile. The light intensity at the receiver displays a nonmonotonic relation as a function of the distance [Fig. 2(b)]. In the far field, the light intensity is inversely proportional to the square of the distance. In the near field, the intensity is governed by the overlap between the emitter and receiver light projections on the surface.

AM transducers are usually used in a distance-measurement range that is limited to only one of the two slopes illustrated in Fig. 2(b). The *front slope* is characterized by a much smaller operating range than that of the *back slope* but also by better sensitivity and accuracy. Moreover, a transducer operating at the front slope is less sensitive to variations in surface-

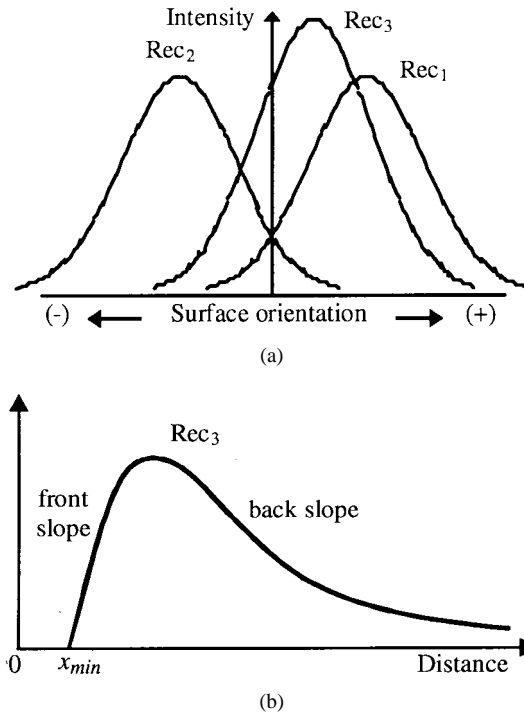


Fig. 2. The light intensity detected as a function of (a) orientation and (b) distance.

reflection characteristics. However, usually, the back slope of the transducer is used in practice, since most proximity-sensor applications require a larger operating range than that achievable using the other.

B. Design of the Proposed Transducer

For its utilization in typical robotic-grasping tasks, the proximity sensor is required to be capable of measuring distances of up to 40 mm, and 2-degree-of-freedom (dof) orientation equivalent to an overall inclination of up to $\pm 30^\circ$ [13]. The use of a single *integrated* transducer, capable of measuring distance as well as orientation, was deemed to be desirable in our work. The use of fiber-optic cables (referred to hereafter simply as fibers) was also noted as beneficial, since they facilitate the operation of sensitive low-noise sensor circuitry in a shielded environment appropriately remote from all electromagnetic-interference sources.

Although, in principle, an AM transducer with one emitter and three receivers is sufficient for extracting the required 3-D information, a transducer with eight receivers is employed herein (Fig. 3). The information provided by the "redundant" measurements is used to obtain a pose-estimation function that minimizes dependency on surface-reflection characteristics. Moreover, the use of eight receivers enables the utilization of both the front and back slopes of the operating range shown in Fig. 2(b).

Because of the minimum operating distance of the AM transducer (x_{\min} in Fig. 2), the transducer must reside a few millimeters away from the contact plane of the robot's gripper. Since the intended principal application of the transducer is to act as a guide for a robot's gripper during the grasping of an object, it was considered highly desirable to have higher

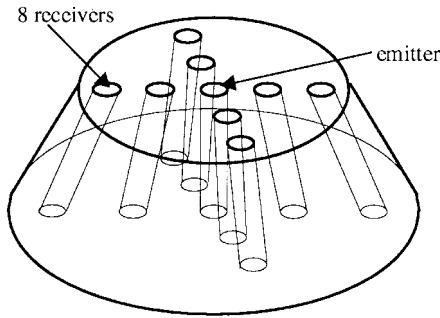


Fig. 3. Geometrical design of the proposed proximity transducer.

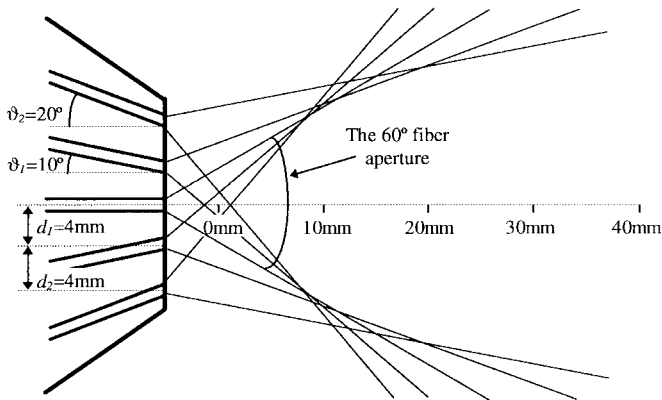


Fig. 4. The AM transducer geometrical design.

sensitivity and accuracy as the gripper approaches the object. Thus, the transducer’s geometrical design was optimized by maximizing the emitter’s and receivers’ light-projections’ overlaps, with respect to the sensitivity and accuracy of the required measurements. The design variables were the angles of the receivers with respect to the transducer’s surface, ϑ_1 , and ϑ_2 , and the distances between adjacent fibers, d_1 , and d_2 in Fig. 1. Fig. 4 illustrates the optimized transducer design.

The fiber selected for use in the transducer was AMP 475-6222. This plastic fiber is commonly used in industrial applications because of its high tensile strength (100N) and its small minimum bend radius (2 cm). It has a 980 μm core diameter, and a 1 mm cladding diameter. The optical attenuation is relatively low at 0.16 dB/m. The numerical aperture is 0.5, and therefore its acceptance angle is $\alpha = 60^\circ$ (Fig. 4).

III. ELECTRONIC INTERFACE CIRCUIT

The performance of an optical transducer is in general limited by its electronic interface. Thus, a robust and reliable computer interface is presented herein for the proximity transducer proposed above. The interface comprises a circuit with one transmitter and eight receivers, built on a PC I/O card, in conjunction with a commercially available controller card (Fig. 5) [14].

It should be noted that, in a typical manufacturing environment, various sources of light noise produce interference in

the visible, near infra-red, and ultra-violet ranges. Noise can be both near-constant and time-varying. Through our interface circuit, optical-noise interference is reduced to less than a measurable level, even in extremely bright “light-infested” surroundings, by utilizing a modulated laser-diode together with optical and electrical filtering.

A necessary requirement for the interface to our transducer is a wide dynamic range. While dynamic range is a very important parameter for any sensor, it is particularly critical for sensors measuring optical attenuation. The light intensity at the receiving end of the proposed transducer is a strong function of many parameters, including distance to the surface, surface orientation, overall reflectivity of the measured surface, and its angular-reflectance profile. As well, at this point, it is important to emphasize that the light-detection process at the receiver involves the conversion of light intensity to current. Therefore, a moderate range of received light intensity of 1000:1, corresponds to a 60 dB electrical-measurement range (rather than to the 30 dB range of optical-power variation).

In practice, the dynamic range of such sensors has, until now, been restricted by the dynamic range of the receiver in the electronic interface. Several sensors incorporate a manual adjustment mechanism that allows varying the operating range of the sensor (without actually increasing the dynamic range) [3]. However, this solution cannot be incorporated into a sensor intended for (automatic) robotic grasping tasks. Our interface-circuit design incorporates a novel method by which this limitation is bypassed and substantial widening of the dynamic range of the sensor system is achieved: The power of the light-source is monitored in a dynamic intensity-control loop designed to perform “floating-point” measurements according to the attenuation found in the associated optical path. By this means, the sensor acquires the combined dynamic ranges of the receiver and transmitter circuits.

The 830 nm wavelength laser diode used as the light source is the Hitachi HL8312G. It is capable of emitting 20 mW of optical power. The current driving the laser diode is composed of a constant biasing current and a 10 kHz modulated intensity current. The received light is detected by an MFOD71 PIN photodiode, which is a low-cost plastic-encased device, designed for direct connection to a 1 mm-core fiber-optic cable. Finally, of the many commercially available controller circuits, the AT-MIO-16 by National Instruments was selected for use in the interface circuit. The AT-MIO-16 is a programmable data-acquisition card for a PC, with 16 analog input channels connected to a 12-b A/D converter, two 12-b D/A output channels, digital I/O, and five counters for timing of I/O operations.

The performance of the electronic-interface circuit was investigated through an analysis of its signal characteristics (including frequency response, noise, sensitivity, dynamic range, and time-domain performance). The results obtained include a receiver dynamic range of 62 dB and an overall dynamic range of 134 dB (when the minimum signal-to-noise ratio is taken to be 10 dB), a receiver input noise of 1.52 $\text{pA}/\sqrt{\text{Hz}}$, and operating-frequency range of 0.5 kHz to 135 kHz. The circuit implemented for our proximity sensor operates at 10 kHz.

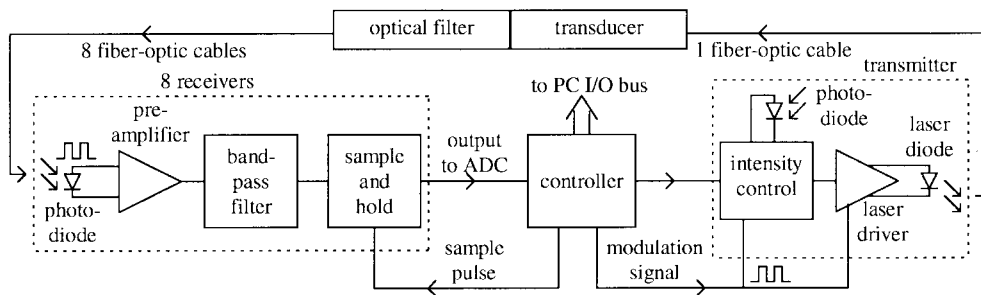


Fig. 5. Electronic-interface circuit block diagram.

IV. SENSOR-CALIBRATION METHODOLOGY

The objective of a calibration process is to establish a reliable relationship between the input and output of a measurement device. In the case of the proximity sensor, the surface pose constitutes the unknown set of parameters to be measured (i.e., the input). The light intensities, collected by the fibers and measured by the interface circuit, constitute the output parameters.

Due to their susceptibility to variations in surface-reflection characteristics, current calibration methods for AM proximity sensors are based on the construction of a calibration-per-surface (CPS) database, and thereby usage of *a priori* knowledge [6], [15], [16]. A single calibration function is obtained for a region that includes the complete operating range of the sensor.

Moreover, due to the unknown reflection characteristics of object surfaces in general, establishing a reliable analytical calibration model has normally been carried out in a decoupled fashion, namely, for the measurement of distance alone or a of single-degree-of-freedom orientation, and only for use in the “far-field” [10]. Therefore, past methods relied on the use of empirical observations for establishing a numerical-analysis-based model. Commonly implemented approaches are polynomial fits, or the combination of polynomial fits and look-up tables.

A new calibration methodology is presented below which increases the robustness of the proximity-sensor measurements, and furthermore, improves its applicability to utilization in active sensing. Three approaches are combined: 1) calibration per group of surfaces; 2) multiregion calibration; and 3) selective-accuracy polynomial fit.

A. Calibration per Group (CPG) of Surfaces

Estimation of the object-surface pose using the CPS approach is a simple process. This approach yields very accurate estimations when the sensor is used for the specific surfaces utilized during calibration. However, the accuracy can decrease rapidly due to lack of uniformity in surface detail, even for objects made of the same material. Thus, the CPS technique is not a practical technique for robotic manufacturing environments.

A CPG technique is proposed herein to address the above robustness problem. Within the framework of this approach, a global relationship is derived for the input/output of the sensor by grouping object-specific data obtained during the

calibration process. A group can be composed of a collection of surfaces made of the same material but with different surface-detail, or surfaces made of different materials but with similar surface-related reflection characteristics.

Although the CPG technique is generally less accurate than the CPS technique for any specific surface utilized during the calibration, it can provide very-comparable estimations as the pose of the surface (relative to the transducer) gets smaller. Also, unlike the CPS technique, the CPG technique considers a variety of materials and surface details. Thus, it can provide acceptable pose estimations for objects that were not included in the original calibration group, but which have similar reflection properties to those of the calibration-group surfaces.

B. Multiregion Calibration

A problem related to the use of a single-region-calibration method is the low achievable accuracy over the complete intended operating range of the proximity sensor. Over this range there exist extensive variations in the light-intensities measured by the eight receivers, variations that are governed by several nonlinear phenomena. Moreover, this type of calibration does not take advantage of the increased accuracy available as the gripper nears the contact point.

Thus, a multiregion-calibration scheme is proposed herein. However, the choice of such a scheme adds another stage to the 3-D-pose-estimation algorithm. While in the case of a single calibration region only one function is needed for estimation, in the multiregion case multiple separate estimations can be made by the different functions. One of three approaches can then be followed.

- 1) Different estimations can be calculated with a reliability factor attached to each. (The reliability factor can be calculated from the relation between the estimated pose and the subregion’s boundaries.) Thereafter, the different estimations can be treated by a sensor-fusion technique as if they were created by different sensors.
- 2) Both the single complete-region and multiregion calibrations can be utilized. The low-accuracy pose estimated by the complete-region calibration can be used to indicate which of the subregion functions should be used for a finer estimation.
- 3) A hybrid hierarchical estimation process can be applied. The first estimation uses a pseudo sensor-fusion technique to select the proper subregion. Thereafter, the

active-sensing algorithm automatically selects the next-smaller subregion as the gripper nears the contact point. Thus, the hierarchical selection of the regions must be arranged such that a sufficiently wide overlap exists between any two adjacent subregions.

C. Empirical Approach

Several different calibration models were evaluated in an effort to find the one that best suits the active-sensing scheme. The result of a *black-box* type approach of symmetrical-polynomial fit proved to be superior to all others, and was thus used for the comprehensive sensor calibration. (Herein, the term “symmetrical-polynomial” indicates that the polynomial possesses both positive and negative powers of the variables.) The estimation errors of the symmetrical-polynomial method were about two to three orders of magnitude lower than those obtained utilizing pseudoanalytical models; about one to two orders of magnitude lower than a hybrid analytical-polynomial-fit model; and about three times lower than an asymmetrical-polynomial-fit method.

The measurements from the eight available receivers are used for the individual estimation of polynomials for x , u , and v (distance, vertical orientation and horizontal orientation). The redundancy in the number of measurements serves to: 1) increase the accuracy of the estimation; 2) reduce the coupling of distance and orientation measurements; and 3) enable the implementation of the CPG scheme.

The data for the calibration process must be acquired via measurements in a 3-D space (x , u and v), defined by the boundaries of each subregion. The measurement points must be suitably distributed in the defined region to achieve an accuracy which is as high as possible. As known, and verified herein, the fit-error decreases as the density of measurement points increases. Thus, in order to optimize the measurement-point selection for the intended use of the proximity sensor in active sensing, a special point-distribution function was developed based on the following criteria: 1) symmetrical pattern for orientation measurements; 2) lower orientation angles as the distance becomes smaller; and 3) increased measurement-point density as the relative distance and orientation between the transducer and the surface become smaller.

The accuracy of the estimation polynomial would naturally rise with the value of r . However, the number of polynomial elements would rise significantly as well, and so would the associated computation cost, both in off-line calculation of the polynomial’s coefficients, and for real-time pose estimation. In our work, the best accuracy-versus-cost performance tradeoff was achieved with $r = 3$ for all the three polynomials.

V. ACTIVE SENSING

A. The Process

At some proximity to the object surface, the control of the robot is released from the medium-range sensing system and passed to the proximity-sensing system. In this context, the operation mode of proximity sensors in estimating the pose of an object’s surface has usually been a direct single-measurement scheme. According to this scheme, the robot’s

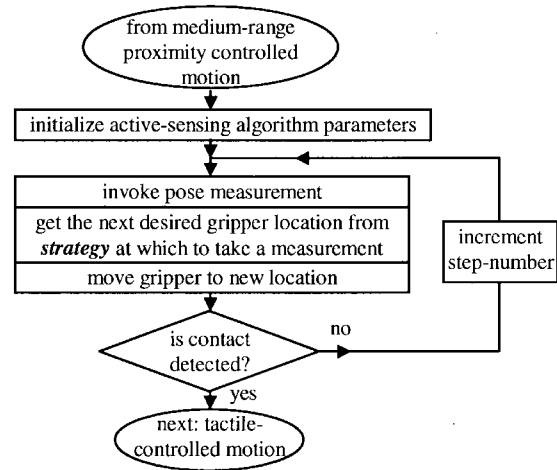


Fig. 6. An active-sensing algorithm.

end-effector is first brought into the proximity of the object to be grasped and a single measurement is taken by the proximity sensor. This measurement is used to estimate the pose of the object’s surface and the gripper is sent there to initiate the grasping process. Active sensing is advocated in this paper as an alternative method. The desired goals for an active-sensing method are:

- 1) at a lower level, to improve the accuracy of the proximity sensor for measurements of precalibrated surfaces;
- 2) at a higher level, to serve the robot motion-control-algorithm with high reliability. This algorithm would control the robot’s micromovements during the pre-grasping stage (that is, from the first proximity-measurement instance until a contact is made between the robot’s end effector and the object’s surface).

Incorporation of an active-sensing algorithm into the process of grasping an object should not significantly lengthen the grasping operation: In practice, it is normally accepted that a robot should be supplied with a new point in its trajectory about every 20 ms. Some of this time is spent in the robot’s controller solving the inverse-kinematics problem. Thus, the active-sensing algorithm must supply a new position for the robot (based on a new pose measurement) in a timeframe which is an order of magnitude faster.

Accordingly, an important requirement for the implementation of such a method is the ability to combine the sensing algorithm with the direct control over the movement of the robot’s end-effector. This would allow the active-sensing algorithm to know the exact pose of the proximity-sensor’s frame while in motion, and thus, to conduct measurements “on the fly.”

The exemplary active-sensing algorithm process, developed for the verification of the proximity sensor proposed herein, was designed as a step-wise execution technique (Fig. 6). The execution of each step starts with the measurement of the light intensities at the eight fibers, and the estimation of the surface pose using calibration data. A strategy algorithm then calculates the next desired gripper location to which the gripper is commanded to move.

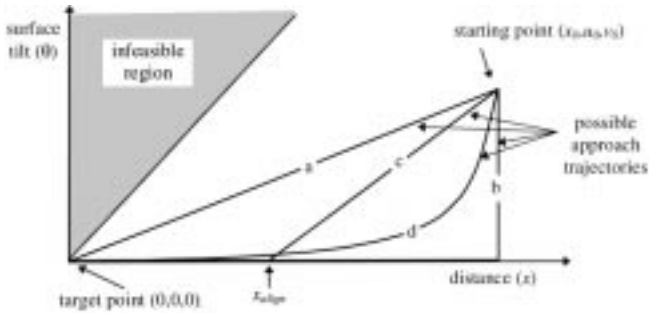


Fig. 7. Possible micromotion robot end-effector trajectories.

B. The Strategy Algorithm

It is assumed herein that contact with the surface should be made when the gripper's surface is aligned with the object's surface, i.e., $(x, u, v) \cong (0, 0, 0)$. An infinite number of possible micromotion trajectories could lead the gripper to this final point from a general starting location, (x_0, u_0, v_0) . Four distinct types of trajectories that can be chosen are shown in Fig. 7. Although many other trajectories may exist, a complete analysis of these possibilities, or exploration of the optimal trajectory for the grasping process, are beyond the scope of this paper.

In Fig. 7, distance to the surface is plotted versus surface tilt, $\theta = \cos^{-1}(\cos u \cdot \cos v)$. Type (a) "linear" trajectory may provide the shortest motion time, however, it does not take advantage of the greater sensor accuracy at smaller values of surface-tilt. Moreover, measurement errors such as overestimating the distance to the surface, would likely result in a surface tilt at the time of contact which is larger than a tilt that results using to other trajectories.

Type (b) trajectory lies at the opposite extreme when compared to a Type (a) trajectory. It is a (premature-contact-wise) safer path since the gripper is first aligned with respect to the surface. However, the execution time of Type (b) trajectory is longer, since two separate motions (including accelerations and decelerations) are carried out sequentially. The two stages of the Type (b) trajectory are referred to as the *align* and *approach* stages.

Type (c) trajectory represents a compromise between (a) and (b). First, the gripper is moved in a "linear" fashion to a predetermined fixed point $(x_{\text{align}}, 0, 0)$, whose distance from the surface is sufficient to prevent premature contact. Then, the approach toward contact with the surface is done along a trajectory in which greater accuracy is available.

Type (d) trajectory represents another potential compromise between (a) and (b). It is fast, continuous and takes some advantage of the greater-accuracy region. The major disadvantage of (d) is the greater complexity in computing a continuous motion.

The active-sensing algorithm's motion strategy need not be constrained to an implementation of only one type of trajectory: A robust algorithm can determine how accurate the pose estimation is after conducting a few measurements, and decide which type of a trajectory should be followed. The estimation accuracy can be checked by comparing the expected measurement values at each point on the trajectory to the actual

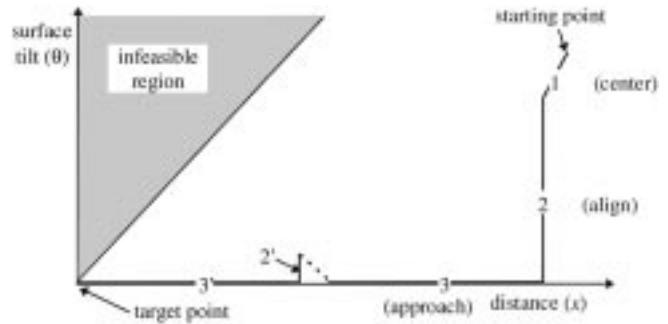


Fig. 8. The modified Type (b) trajectory implemented in the active-sensing algorithm.

value measured. High accuracy indicates that the calibration data being used matches well the surface properties, and a fast trajectory can be adopted. On the other hand, low accuracy indicates improper calibration data, and a safer and that a more conservative trajectory should be used for approaching the object's surface.

The strategy algorithm implemented in our research was based on Type (b) trajectory. However, for its adaptation into a multiregion calibration environment, the trajectory-planning scheme was modified to include a *centering* motion in addition to the *align* and *approach* motions. Also, the algorithm was designed such that it can decide to take any one of the three stages as it nears the object and the sensor switches from one calibration region to another (Fig. 8). Each motion may include several steps (see the Appendix).

VI. EXPERIMENTS

A. Setup

An experimental setup was developed for fully-automatic measurement-acquisition control and object-surface-motion control (Fig. 9) [13]. In this setup, the "real world" six degrees-of-freedom (6-dof) gripper motion was simulated by a 3-dof motion of the object, specifically, distance to the sensor (x), and vertical (u) and horizontal (v) orientations of the surface normal relative to the sensor's surface normal. The implemented simulation algorithm considered the imperfect positioning of the sensor/gripper, as it would actually occur in the real world due to previous pose-estimation errors, and placed the object accordingly.

B. Calibration Results

Experiments were conducted to compare the accuracy achieved by the CPG and CPS methods using various materials. Individual CPS calibrations were first carried out for referencing purposes for aluminum, copper, brass, stainless-steel, Teflon, PVC, wood, and Plexiglas surfaces. These materials were then classified into two separate groups, namely metals and dielectrics, and CPG calibrations were conducted on these groups. Finally, all the materials were combined into a single group and an overall general calibration (GC) was obtained.

TABLE III
ESTIMATION-ERRORS' $\mu \pm \sigma$ IN THE FINE REGION FOR UNCALIBRATED SURFACES

variable	method	$\mu_x \pm \sigma_x$ (mm)	$\mu_u \pm \sigma_u$ (°)	$\mu_v \pm \sigma_v$ (°)
galvanized steel	GC	-0.21±0.31	0.09±0.58	0.34±0.64
	CPG - metals	-0.07±0.24	-0.38±0.24	-0.48±0.41
white paper	GC	0.53±0.45	-3.42±0.63	1.89±0.29
	CPG - dielectrics	0.20±0.25	-3.77±1.14	1.26±0.54
aluminum-2	GC	0.59±0.26	-0.41±0.51	0.12±0.45
	CPG - metals	0.92±0.19	-0.71±0.22	-0.23±0.28
	CPS - aluminum	-1.43±3.78	8.63±10.7	7.34±4.13

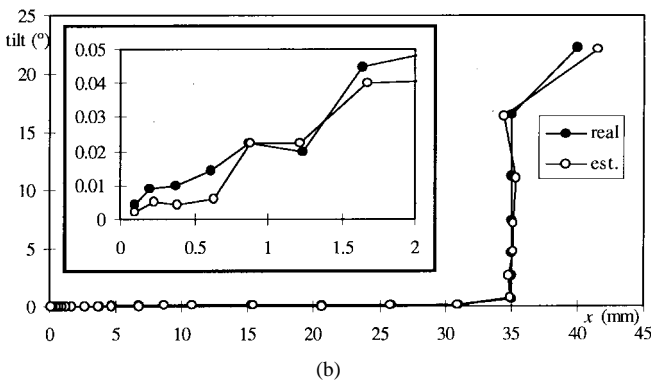
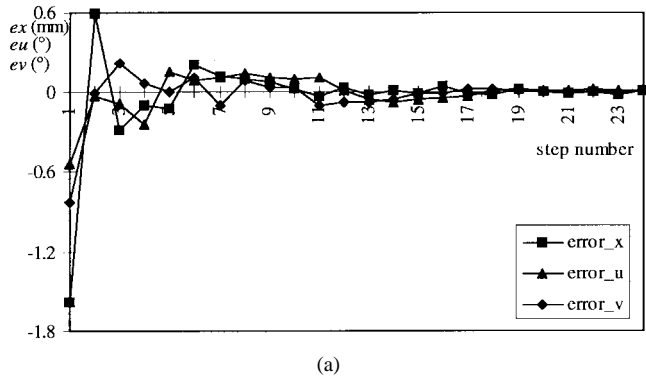


Fig. 11. Active-sensing grasping of a teflon surface. (a) Estimation errors. (b) Real and estimated trajectories.

ulation subsets, which are composed of the samples of a single surface. This bias is a measure of the uniformity of reflection characteristics inside a group, and, particularly, a measure of how far the reflection characteristics of a surface deviate from the group's average. Correspondingly, this property may assist in the categorization of surfaces into groups.

The validity of the observed results was verified as follows: Additional (and independent) random sample sets of 70 measurements were obtained, for every material and subregion, at different poses than those used for the calibration. Again, the estimation-errors were analyzed. Both the means and standard deviations of the samples' errors were within the statistical limits calculated from the basic calibration results according to Sampling Theory [17].

C. Uncalibrated Surfaces

This section describes work intended to explore the possibility of using the CPG-scheme calibration for pose es-

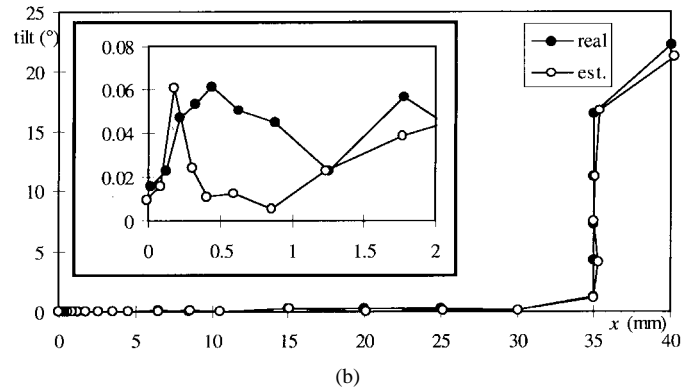
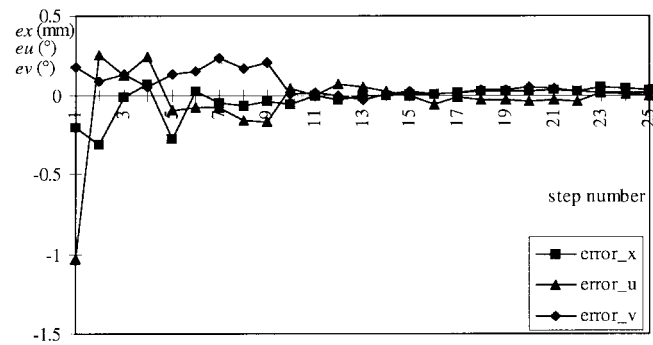


Fig. 12. Active-sensing grasping of a brass surface. (a) Estimation errors. (b) Real and estimated trajectories.

timations on surfaces that are not included in the original group. Experiments were conducted with two new materials (galvanized steel and white paper), and with an aluminum sample (aluminum-2) having a surface-roughness different than the one used in the previous experiments. Measurement points obtained for these materials were gathered with the same distribution parameters used in the previous experiments (1960 points).

By way of an example, the estimation-errors' means and standard deviations for the fine region are given in Table III. Estimation errors in other regions display the same relative accuracies as given in Table II. The results can be used to compare the performance of the GC, CPG-metals, CPG-dielectrics, and CPS-aluminum with respect to the new materials.

The following three points summarize our observations.

- 1) The estimations of CPG/CG can permit effective pose-estimation of uncalibrated surfaces.
- 2) In the case of the same material but different surface roughness, "aluminum" versus "aluminum-2," the estimation accuracies of CPG/CG are better than these of the CPS technique, where for the latter we used a calibration function developed for "aluminum" during the pose estimation of the "aluminum-2" surface object.
- 3) The aluminum-2 object cannot be grasped in an active-sensing process based on the CPS-aluminum calibration function since the pose-estimation errors are larger than the region dimensions (as seen in Table III for the fine region).

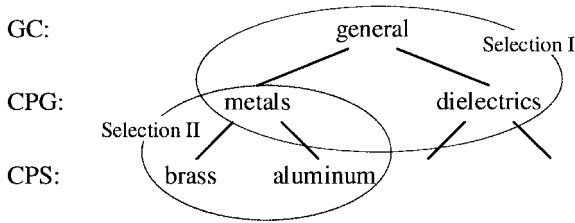


Fig. 13. Hierarchical selection of the calibration function.

D. Active-Sensing Results

Exemplary and typical active-sensing grasping processes are illustrated in Figs. 11 and 12, for Teflon and brass surfaces, respectively. Each figure illustrates: (a) the estimation errors of the surface pose and (b) the real and estimated trajectories of the active-sensing process with a magnified inset of the last few steps. In each case, the gripper was brought to contact with the surface from a starting location $(x_0, u_0, v_0) = (40 \text{ mm}, -20^\circ, 10^\circ)$. The final measurement errors (e_x, e_u, e_v) were $(0.004 \text{ mm}, 0.003^\circ, 0.006^\circ)$ and $(0.03 \text{ mm}, -0.008^\circ, 0.013^\circ)$, for the teflon and brass surfaces, respectively. The grasping process of other calibrated materials followed the same pattern, and yielded comparable results.

Contact with the uncalibrated surfaces used in the experiments was reached at surface tilt of $0.4^\circ, 0.6^\circ,$ and 1.2° using CPG, and at surface tilt of $0.5^\circ, 0.6^\circ,$ and 1.4° using GC for galvanized steel, aluminum-2, and white paper surfaces, respectively.

E. Selection of the Calibration Function

In general, when there is no *a priori* knowledge of the object to be grasped, the lower accuracy GC calibration must be used. However, a hierarchical surface-recognition method can be applied for the automatic selection of the calibration function to be used for pose estimation: first, the surface group is selected, and then the specific surface itself is chosen (Fig. 13).

The results of an experiment conducted to explore this possibility are given in Table IV. First, the position of an unknown surface was estimated using GC, CPG-dielectrics, and CPG-metals methods: 23.86, 54.26, 25.28 mm, respectively, (versus, the real distance of 30 mm). (The first row in Table IV lists other estimates for referencing purposes). Next, the gripper was advanced 5 mm toward the surface and a second estimation was once again carried out using GC, CPG-dielectrics and CPG-metals methods: 20.45, 58.25, and 21.27 mm, respectively. Once a decision was made on the type of material as “metals,” a finer estimation was obtained using the individual CPS-type calibration functions within the group. As noted in Table IV, the calibration function of brass *correctly* provided the best match.

TABLE IV
SELECTION OF THE PROPER CALIBRATION
FUNCTION BASED ON A SINGLE x MOVEMENT

calibration function	general	dielectrics	metals	brass	aluminum
first estimation at (30mm,10°,10°)	23.86	54.26	25.28	30.87	18.9
second estimation at (25mm,10°,10°)	20.45	58.25	21.27	25.68	16.06
estimation difference (mm)	3.41	-3.99	4.01	5.19	2.84

VII. CONCLUSION

In this paper, a new amplitude-modulation-based proximity sensor that combines several novel features has been presented. The primary objective of the development was to obtain a robust proximity sensor for utilization in robotic active-sensing tasks.

The new AM proximity transducer uses redundant measurements to improve the robustness of the sensor. The transducer design was optimized to provide increased robustness and increased measurement accuracy as the gripper nears the contact point. A novel electronic interface circuit was designed to provide the required extended dynamic measurement range for the utilization of the proximity sensor in an active-sensing environment. The circuit’s protective mechanisms against light noise allows operation of the sensor in typical manufacturing environments.

The features of the AM transducer allow the utilization of a new CPG of surfaces methodology. This methodology was employed in an attempt to address the problem of robustness of AM proximity sensors to surface-reflection characteristics. The sensor was calibrated individually for eight different materials using CPS, as well as globally for all eight materials and for two groups of materials (metals and dielectrics) using CPG.

The potential application of the proposed proximity sensor in controlling the micromovements of a robot’s gripper was explored by a prototype active-sensing algorithm. The combination of active sensing and the proposed multiregion calibration improves the grasping accuracy by more than an order of magnitude in comparison with a single-measurement scheme. Physical experiments verified the expected good performance of the CPG-calibrated proximity sensor for all the *a priori* considered surfaces, as well as for surfaces not considered before.

APPENDIX

Motion step sizes were calculated in our active-sensing algorithm individually for each axis, and differently for the three possible stages of motion. As expected, the steps are larger at the beginning of the motion, and become smaller as the gripper nears the end of the specific motion stage.

The x -axis-displacement step size is calculated as

$$\text{step}_x = \max(\text{step}_{x_{\min}}, \min(x \cdot \text{ratio}_x, \text{step}_{x_{\max}})) \quad (\text{A1})$$

$$\text{step}_\alpha = \begin{cases} -\max(\text{step}_{\alpha_{\min}}, \min(-\alpha \cdot \text{ratio}_\alpha, \text{step}_{\alpha_{\max}})) & -\alpha > \alpha_0 \\ \alpha & |\alpha| \leq \alpha_0 \\ \max(\text{step}_{\alpha_{\min}}, \min(\alpha \cdot \text{ratio}_\alpha, \text{step}_{\alpha_{\max}})) & \alpha > \alpha_0 \end{cases} \quad (\text{A2})$$

where $\text{step}_{x_{\min}}$ and $\text{step}_{x_{\max}}$ are user-set minimum and maximum limiting values, and ratio_x provides a constant fraction of the distance to the object.

Similarly, the u - and v -axis-displacement step sizes are calculated as shown in (A2) at the bottom of the previous page, where for $\alpha = u, v$, $\text{step}_{\alpha_{\min}}$ and $\text{step}_{\alpha_{\max}}$ are user-set minimum and maximum limiting values, ratio_{α} is a constant step ratio, and α_0 is an alignment criterion for u or v .

The values of the above-mentioned parameters are defined separately for each of the calibration subregions. The maximum-step-size limits are needed in order to prevent premature contact due to an erroneous estimation of the surface pose. The minimum-step-size limits are needed in order to ensure a finite approach process, and to limit the slow-down of the gripper approach toward contact.

REFERENCES

- [1] B. Espiau, "An overview of local environment sensing in robotics applications," *Sensors and Sensory Systems for Advanced Robots, NATO ASI Series*, Berlin, Germany, vol. F43, pp. 125–151, 1988.
- [2] A. Bradshaw, "Sensors for mobile robots," *Measure. Contr.*, vol. 23, no. 2, pp. 48–52, Mar. 1990.
- [3] R. Volpe and R. Ivlev, "A survey and experimental evaluation of proximity sensors for space robotics," in *IEEE Int. Conf. Robot. Automat.*, San Diego, CA, Mar. 1994, vol. 4, pp. 3466–3473.
- [4] S. Lee and J. Desai, "Implementation and evaluation of HexEYE: A distributed optical proximity sensor system," in *IEEE Int. Conf. Robot. Automat.*, Nagoya, Japan, May, 1995, vol. 3, pp. 2353–2360.
- [5] S. Lee and H. Hahn, "Recognition and localization of 3-D natural quadric objects based on active sensing," in *IEEE Int. Conf. Robot. Automat.*, Sacramento, CA., Apr. 1991, vol. 1, pp. 156–161.
- [6] O. Partaatmadja, B. Benhabib, E. Kaizerman, and M. Q. Dai, "A two-dimensional orientation sensor," *J. Robot. Syst.*, vol. 9, no. 3, pp. 365–383, 1992.
- [7] H. Kopola, S. Nissilä, R. Myllylä, and P. Kärkkäinen, "Intensity modulated fiber optic sensors for robot feedback control in precision assembly," in *SPIE, Fiber Optic Sensors II*, vol. 798, Mar. 1987, pp. 166–175.
- [8] H. B. Gurocak and A. de Sam Lazaro, "A method of position sensing for precision assembly," in *3rd ASME Conf. Flexible Assembly Syst.*, Miami, FL, Sept. 1991, vol. DE-33, pp. 49–56.
- [9] B. Allotta and G. Buttazzo, "Impact handling by proximity and force sensing," in *IEEE Int. Conf. Robot. Automat.*, Nice, France, May 1992, vol. 3, pp. 12–14.
- [10] Y. F. Li, "Characteristics and signal processing of a proximity sensor," *Robotica*, vol. 12, no. 4, pp. 335–341, July 1994.
- [11] ———, "A proximity sensor and its application in real-time robot control," *Robot. Autonomous Syst.*, vol. 13, no. 1, pp. 25–37, June 1994.
- [12] P. P. L. Regtien, "Accurate optical proximity detector," in *IEEE Conf. Instrum. Measure. Technol.*, San Jose, CA, Feb. 1990, pp. 141–143.
- [13] A. Bonen, "Development of a robust electro-optical proximity-sensing system," Ph.D. dissertation, Dept. Elect. Comput. Eng., Univ. Toronto, Oct. 1995.
- [14] A. Bonen, R. E. Saad, B. Benhabib, and K. C. Smith, "A novel optoelectronics interface-circuit design for sensing applications," in *IEEE Conf. Instrum. Measure. Technol.*, Boston, MA, Apr. 1995, pp. 658–663.
- [15] O. Partaatmadja, B. Benhabib, and A. A. Goldenberg, "Analysis and design of a robotic distance sensor," *J. Robot. Syst.*, vol. 10, no. 4, pp. 427–445, June 1993.
- [16] H. Kopola, S. Nissilä, R. Myllylä, and P. Kärkkäinen, "Intensity modulated fiber optic sensors for robot feedback control in precision assembly," in *SPIE, Fiber Optic Sensors II*, vol. 798, Mar. 1987, pp. 166–175.
- [17] R. E. Walpole and R. H. Myers, *Probability and Statistics for Engineers and Scientists*. New York: Macmillan, 1993, 5th ed.



Adi Bonen was born on November 3, 1973, in Israel. He received the B.Sc. degree (summa cum laude) in electrical engineering from the Technion, Israel Institute of Technology, in 1990. He received the Ph.D. degree in 1995 from the Department of Electrical and Computer Engineering, University of Toronto.

During 1992–1993, he was on a research-internship program with the Hitachi Central Research Laboratories, Tokyo, Japan, working on an optical computed tomography system. His current research interests include electrooptical measurements, robotic sensors, and sensing technologies.



Ricardo E. Saad received the electrical engineering Diploma with first-class honors from the National University of Cordoba, Argentina, in 1986, and the M.Sc. degree with distinction award in electrical engineering from the State University of Campinas, Brazil, in 1989. He received the Ph.D. degree from the Department of Electrical and Computer Engineering, University of Toronto, Ontario, Canada, in 1996.

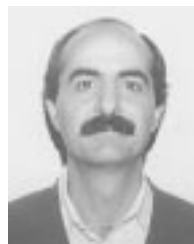
From 1987 to 1990, he was with the Optoelectronics Device Department, Research Center, Brazilian Telecommunication Holding Company. He is currently with the Department of Electrical and Computer Engineering, University of Toronto. His research interests are in robotic sensing, optical sensing, optoelectronics, and microwave and optical communications.



Kenneth Carless Smith (S'53–A'54–M'60–M'76–F'78–LF'96) received the Ph.D. degree in solid-state physics from the University of Toronto, in 1960.

Currently, he is a Professor of electrical and computer engineering, mechanical and industrial engineering, computer science, and information studies at the University of Toronto. He is also a Visiting Professor with the Department of Electrical and Electronic Engineering, Hong Kong University of Science and Technology. His research interests currently include analog VLSI, multiple-valued logic, sensor systems, machine vision, instrumentation, array architectures, human factors and reliability. He is widely published in these and other areas, with more than 200 journal and proceedings papers, books, and book contributions.

He was elected Fellow of the IEEE in 1978 for "Contributions to Digital Circuit Design," and made Life Fellow in 1996.



Beno Benhabib (M'93) received the Ph.D. degree in mechanical engineering from the University of Toronto, in 1985.

He is currently a Professor and Associate Chair with the Department of Mechanical and Industrial Engineering, University of Toronto. His research interests are in the general area of computer-integrated manufacturing. His work has been published on various aspects of robot-motion planning, machine vision, robotic sensors, and supervisory-control of manufacturing systems. He has been a consultant to various Ontario manufacturers in the areas of CAD/CAM, robotics, and automated quality control.

Dr. Benhabib is a senior member of the SME and a member of the ASME. He is a registered Professional Engineer.